

AN OPTIMIZED ENERGY-EFFICIENT PATH FOLLOWING ALGORITHM FOR UNDERACTUATED MARINE SURFACE SHIP MODEL

(DOI No: 10.3940/rina.ijme.2018.a4.505)

Haitong Xu and **C Guedes Soares** Centre for Marine Technology and Ocean Engineering (CENTEC), Instituto Superior Técnico, Universidade de Lisboa, Portugal

SUMMARY

An optimized path following guidance law is proposed for path-following of an underactuated surface ship. The main purpose of the proposed guidance law is to make a marine vessel travel with more energy efficiency. A combined feedback and feedforward controller is used for the heading control. The feedforward term is designed based on the well-known Nomoto model, whose parameters are estimated using least-square support vector regression. In order to achieve optimal operation of a marine vessel, a global optimization algorithm is employed to search the regularization factors, which are the trade-off between the total cross-track errors and total control energy. The simulation studies are carried out to demonstrate the performance of the proposed guidance law. The proposed method is an effective and practical guidance law and provide an optimal option for marine navigator.

NOMENCLATURE

ψ_d	Desired heading angle (°)	e_i	Error variables
ψ_{pp}	Desired heading angle calculated by PP (°)	C	Regularization factor
ψ_{los}	Desired heading angle calculated by LOS (°)	$K(\cdot, \cdot)$	Kernel function
τ	Distance of transition region (m)	τ_N	Controller yaw moment ($\text{kg}\cdot\text{m}^2\cdot\text{s}^{-2}$)
(x_{los}, y_{los})	Coordinate of the LOS vector	τ_{FF}	Feedforward term of yaw moment ($\text{kg}\cdot\text{m}^2\cdot\text{s}^{-2}$)
y_e	Cross-track error (m)	ω_n	Natural frequency (s^{-1})
(w_{xj}, w_{yj})	waypoints	ζ	Relative damping ratio
(x, y)	Current location of the ASV	$K_{p,j,d}$	controller gains
d	Distance from the waypoint j+1 (m)		
ρ	Sign of cross-track error ($\text{kg}\cdot\text{m}^{-3}$)		
L	Length between perpendiculars (m)		
$F_i (i=1,2)$	Defined cost function		
$\tilde{\delta}_R$	Normalized ruder angle		
\tilde{y}_e	Normalized cross-track error		
u	Surge speed in body frame ($\text{m}\cdot\text{s}^{-1}$)		
v	Sway speed in body frame ($\text{m}\cdot\text{s}^{-1}$)		
u_r	Relative surge speed ($\text{m}\cdot\text{s}^{-1}$)		
v_r	Relative sway speed ($\text{m}\cdot\text{s}^{-1}$)		
u_c	Current velocity ($\text{m}\cdot\text{s}^{-1}$)		
α	Current direction (°)		
\dot{u}_r	Acceleration of surge ($\text{m}\cdot\text{s}^{-2}$)		
\dot{v}_r	Acceleration of sway ($\text{m}\cdot\text{s}^{-2}$)		
\dot{j}	Acceleration of yaw ($\text{rad}\cdot\text{s}^{-2}$)		
$f_i (i=1\cdots 3)$	Forces and moment of surge, sway and yaw ($\text{kg}\cdot\text{m}\cdot\text{s}^{-2}$, $\text{kg}\cdot\text{m}^2\cdot\text{s}^{-2}$)		
ρ	Density of water ($\text{kg}\cdot\text{m}^{-3}$)		
n	RPS of propeller		
C_R	resistance coefficient		
S	wetted surface area (m^2)		
c	Weighted average flow speed ($\text{m}\cdot\text{s}^{-1}$)		
b	Bias term		
w	weight matrix		
$\Phi(\cdot)$	Nonlinear mapping function		

1. INTRODUCTION

Autonomous marine vehicles have been widely used both in navy and commercial applications recently, such as marine survey, environment monitoring, marine rescue, *et. al.* In 2017, International Maritime Organization (IMO) have added Autonomous Ships to its agenda and now starts mapping how existing international regulations can be applied to autonomous ships. Autonomous surface vehicles (ASV) have been playing an important role in the last decade due to their advantages. For autonomous vehicles, guidance systems are critically important, because they are concerned with the transient motion behaviour associated with the achievement of motion control objectives (Breivik and Fossen, 2009).

Path following is one of typical problems for guidance law and control (Lekkas and Fossen, 2014). The object is to control the ship to follow a predefined path, which is usually defined by way-points (Fossen, 2002). The way-points are given by the marine navigator considering some features such as weather conditions (Vettor and Guedes Soares, 2015), sea states (Chen, et al. 2013), obstacle avoidance (Perera et al, 2011), mission, and control effort. In most cases, a straight line is used to connect the way-points (Fossen, 2011), but due to the discontinuity on the 1st order derivative, some methods, have been used to generate smooth path, such as polynomial, Dubins path (Fossen et al., 2015), and CHSI (Lekkas and Fossen, 2014).

Conventional ships are usually underactuated systems, since there is not enough control input corresponding to the degrees of freedom. In most cases, the conventional surface ship is equipped with one propeller for speed control and rudders for heading control (Fossen et al., 2003). This minimum configuration for path-following control is one typical underactuated problem (Sutulo and Guedes Soares, 2005). This means that only two controls are available, thus rendering the ship underactuated for the task of 3 degree of freedom (surge, sway, and yaw) tracking control.

Line-of-Sight (LOS) is a well-known guidance law for autonomous surface vehicles. Moreira, et al. (2007) presented a dynamic LOS for autonomous ship, further extended in (Moreira and Guedes Soares, 2011a). The vector field is a promising method for guidance problems of Unmanned Aerial Vehicles (Lim, et al. 2014). It is a simple and stable method for UAV (Frew et al. 2008). Lim, et al. (2014), extended the vector field method to control the arrival position, angle and time. Vector field guidance law also has been used for autonomous marine vehicles. The time-varying ocean disturbances were considered for the path-following of marine surface vehicles (Liu et al., 2016a), and further developments can be found in (Liu et al., 2016b). The effect of surge speed was studied in (Wang et al., 2017). Caharija et al. (2015), applied the vector field to solve the guidance problem of autonomous underwater vehicle. Xu and Guedes Soares, (2016), discussed the parameters of the vector field in details, and the stability is also proved using Lyapunov stability theory.

The classical path-following guidance law usually focuses on minimising the cross-track errors. But it is not practical in real applications especially when the ship is far away from the desired path. The traditional LOS will turn the ship directly perpendicularly to the path. This route is usually with the smallest cross-track errors, but it is not a practical one because it will cost more energy and this is not wise for an ASV, which should be energy-efficient vessels due to the limited energy onboard and the need of automatic collision avoidance systems (Jingsong et al., 2008).

The contribution of this paper is to design an ASV's control system based on a waypoint guidance algorithm using pursuit and line of sight (PLOS), which is used to compute the desired heading angle. The PLOS is a combination of the pure pursuit and LOS with different gain, which is optimized by using a genetic algorithm. The PLOS will make the vehicles follow the path with a trade-off between the total cross-track errors and control efforts. Simulation tests based on the mathematical model of the ASV are carried out to compare the performance of the PLOS with the traditional LOS.

2. GUIDANCE LAWS FOR PATH FOLLOWING

Guidance systems are very important for autonomous surface vehicles. The methods used widely by the marine control community have been influenced by their missile community counterparts, such as the line of sight guidance and the pure pursuit guidance. In this section, the principles of guidance laws for path following are briefly introduced. An optimal guidance law is proposed based on a global optimization algorithm.

The line of sight guidance law was widely used in the path following control scenario of autonomous surface vehicles (Breivik and Fossen, 2008). As presented in Figure. 1, the LOS guidance law computes a vector from the ship to the virtual target point (VTP). The vector represented the desired heading angles. The ship will converge to the predefined path when it follows the desired heading angle. The LOS guidance law is very simple and easily to implement, but the drawback with a LOS vector pointing to the VTP is that the ship located far away from the path will result in large cross-track errors in presence of wind, current and wave disturbances (Moreira, et al. 2007). The constant force generated by wind or current will offset the force generated by the LOS algorithm and this will result on a large control effort and waste much energy.

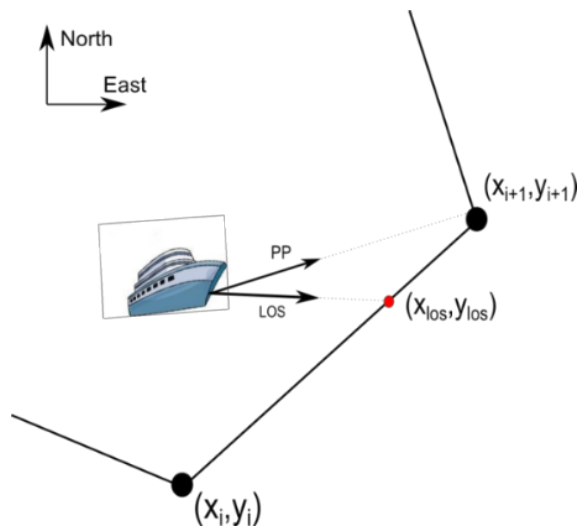


Figure 1. The classical guidance laws line of sight (LOS) and pure pursuit (PP)

Pure Pursuit (PP) is one typical well-known two-point guidance schemes. It is inspired by a predator chasing a prey in the animal world, and very often results in a tail chase (Breivik and Fossen, 2008). As presented in Figure. 1, PP guidance law can always control the ship passes the predefined waypoints with a minimum control effort however, the drawback is obviously that it is usually with large cross-track errors. It has been widely used for air-to-surface missile (Zarchan, 1990).

As discussed above, a new guidance law can be proposed by combining the pure pursuit and LOS guidance law. This guidance law can also be called pure pursuit and LOS guidance law (PLOS) (Zarchan, 1990). This choice is motivated from the fact that the LOS steers the vehicles to follow the path and the pure pursuit allows the vehicles to reach the desired waypoint (Xu and Guedes Soares, 2015; 2016b). The PLOS is defined by Eq. 1. The regularization factor is a trade-off between the total cross-track errors and control efforts. The geometry of the vehicle and the path are presented in Figure 2.

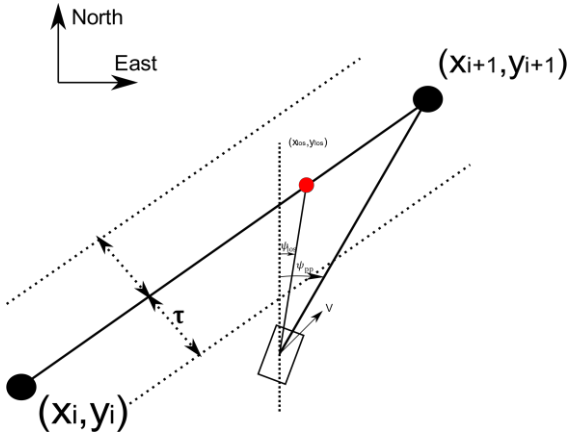


Figure 2. PLOS guidance geometry for straight line

$$\psi_d = \begin{cases} p \cdot \psi_{los} + q \cdot \psi_{pp} & \text{if } y_e > \tau \\ \psi_{los} & \text{if } y_e \leq \tau \end{cases} \quad (1)$$

where, ψ_d is the desired heading angle, p and q are the regularization factors. The first term is calculated by LOS guidance law, and the second term is the contribution by pure pursuit guidance law, which guides the ASV towards the waypoint.

$$\psi_{pp} = \text{atan2}(y_{i+1} - y, x_{i+1} - x) \quad (2)$$

$$\psi_{los} = \text{atan2}(y_{los} - y, x_{los} - x) \quad (3)$$

where (x_{los}, y_{los}) is the virtual target point, which is calculated by the equation (4) and (5).

$$(x_{los} - x)^2 + (y_{los} - y)^2 = (nL_{pp})^2 \quad (4)$$

$$\frac{y_{los} - y_{k-1}}{x_{los} - x_{k-1}} = \frac{y_k - y_{k-1}}{x_k - x_{k-1}} = \text{cont.} \quad (5)$$

From equation (1), the design parameter p and q has an important effect on the performance of the PLOS guidance law. In order to get the optimal parameters, a global optimisation evolutionary algorithm is employed to do global-search for the best values. Genetic algorithm inspired by Darwin's theory about evolution (Melanie, 1996) is applied to minimise the cost functions with the following base parameters: the generations was 50, the populations counted 30 individuals, the crossover rate is 0.9 and the single-bit mutation is 0.1. The generations

and populations are chosen considering the convergence speed. In this problem, there are two parameters that need to be optimized and thus it is not necessary to choose large populations and generations. The work flow of a classical genetic algorithm is presented in Figure.3.

Firstly, the cost function needs to be defined. Most path-following algorithms focus on minimizing the cross-track errors, but this will increase the control effort in most cases especially when the vehicles are far away from the path, which is not desired for autonomous surface vehicle owing to its limited energy. Too much steering of the ship inevitably leads to the over-shoots and wiggly paths, which costs extra energy and should be avoided for the autonomous vehicles. In order to minimise the control effort with certain cross track errors permission, two metrics are defined here: total control effort and total cross-track error. The total control effort quantifies the control demands of the guidance law. If the solutions take too many turns, then control effort will be high. The total cross-track error is the offset of the vehicle from the desired path (Sujit, et al. 2014). The cost function is

$$F_1 = \sum_{t=0}^{t=T} \tilde{\delta}_R^2 + \sum_{t=0}^{t=T} \tilde{y}_e^2 \quad (6)$$

$$F_2 = \sum_{t=0}^{t=T} \tilde{\delta}_R^2 + \sum_{t=0}^{t=T} \tilde{y}_e^2 + \sum_{t=0}^{t=T} (\tilde{\psi}_r - \tilde{\psi}_d)^2 \quad (7)$$

In equation (6), the function defined to minimise the total ruder angle and total cross track errors. In equation (7), an extend version considering the heading error was proposed.

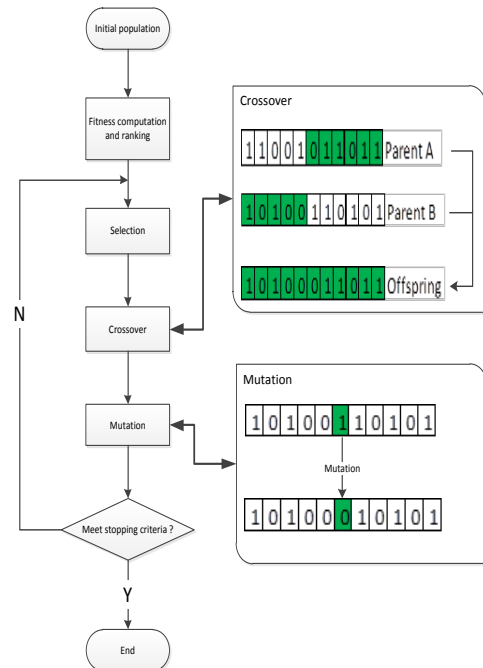


Figure 3: The work flow of a classical genetic algorithm

3. MANOEUVRING SIMULATION OF UNDERACTUATED SURFACE SHIP AND PARAMETER IDENTIFICATION

In this section, manoeuvring simulation will be carried out using “Esso Osaka” ship model (Figure.4). The guidance and control program were programmed and tests of ASV were carried out by Perera, et al. (2012, 2015). The model was scaled 1:100 from the real ship (Moreira and Guedes Soares 2011b; Xu et al. 2018). It is a typical underactuated ship model, because, it is equipped with fewer independent actuators than the degrees of freedom. It means that the surge and yaw can be controlled directly, but there is no control force for sway motion. The principal dimensions of the model are listed in Table 1 and the nondimensionalize hydrodynamic coefficients, which are used to simulate the “Esso Osaka” trial manoeuvres (Sutulo et al. 2002), are presented in Table 2.

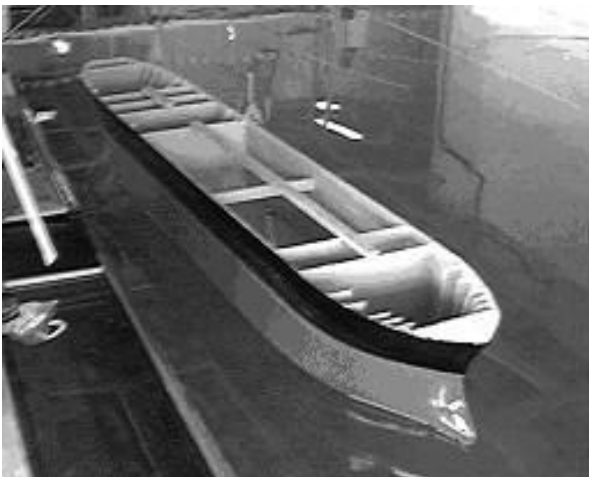


Figure 4. The “Esso Osaka” ship model

In order to make the modelling more flexible and physically more realistic, the classical nonlinear Abkowitz model has been modified by including the rotation speed of the propeller and the flow velocity over rudder. The flow velocity over rudder was used to nondimensionalize the forces and moment induced by rudder deflection, due to the complicated fluid region around the rudder.

Table 1. The principal dimensions of “Esso Osaka” ship model

Parameter	Value	Unit
Length overall	3.430	m
Length between perpendiculars (L)	3.250	m
Breadth	0.530	m
Draft	0.217	m
Block coefficient	0.831	
Number of rudders	1	
Rudder area	0.0120	m ²
Propeller area	0.0065	m ²
Longitudinal CG	0.103	m
Displacement	319.40	kg

The current effect is considered to be the main external excitation owing to the small above water structure. The manoeuvring model will be the one presented in Abkowitz (1980)

$$\begin{cases} u_r = u - u_c \cos(\psi - \alpha) \\ v_r = v - u_c \sin(\psi - \alpha) \end{cases} \quad (8)$$

Table 2. The nondimensionalized hydrodynamic coefficients of “Esso Osaka” ship model

Coefficient	Value	Dimensional Factor	Coefficient	Value	Dimensional Factor
$(m - Y_v)'$	0.0352	$0.5\rho L^3$	Y'_{vrr}	0.00611	$0.5\rho L^4 U_r^{-1}$
$(I_z - N_r)'$	0.00222	$0.5\rho L^5$	X'_{ee}	-0.00224	$0.5\rho L^2 c^2$
Y'_v	-0.0261	$0.5\rho L^3$	X'_{rvv}	-0.00715	$0.5\rho L^4 U_r^{-2}$
Y'_r	0.00365	$0.5\rho L^3 U_r$	N'_{eee}	0.00116	$0.5\rho L^2 c^2$
N'_v	-0.0105	$0.5\rho L^3 U_r$	Y'_{vrr}	-0.0450	$0.5\rho L^2 U_r$
Y'_r	-0.00480	$0.5\rho L^3 U_r$	η'_1	-0.962×10^{-0}	$0.5\rho L^2$
Y'_δ	-0.00283	$0.5\rho L^2 U_r^2$	η'_2	-0.446×10^{-0}	$0.5\rho L^3$
$X'_{vy} + m'$	0.0266	$0.5\rho L^3$	η'_3	0.0309×10^{-0}	$0.5\rho L^4$
N'_0	-0.00028	$0.5\rho L^3 (u_{Aoc}/2)^2$	m'	0.0181	$0.5\rho L^3$
			C'_R	0.00226	$0.5\rho S u_r^2$

The resulting advance speed of the vehicle is given by

$$U_r = \sqrt{u_r^2 + v_r^2} \quad (9)$$

The derivative with respect to time of u and v are given by the following expressions:

$$\begin{cases} \dot{u} = \dot{u}_r - u_c r \sin(\psi - \alpha) \\ \dot{v} = \dot{v}_r - u_c r \cos(\psi - \alpha) \end{cases} \quad (10)$$

where

$$\begin{cases} f_1 = \eta_1 u_r^2 + \eta_2 n u_r + \eta_3 n^2 - C_R + X_{v_r}^2 v_r^2 + X_{e^2} e^2 + (X_{r^2} + m x_G) r^2 + (X_{v_r r} + m) v_r r + X_{v_r^2 r^2} v_r^2 r^2 \\ f_2 = Y_0 + \{Y_{v_r} v_r + Y_{\delta} (c - c_0) v_r\} + \{(Y_r - m u_r) r - \frac{Y_{\delta}}{2} (c - c_0) r\} + Y_{\delta} \delta + Y_{r^2 v_r} r^2 v_r + Y_{e^3} e^3 \\ f_3 = N_0 + \{N_{v_r} v_r - N_{\delta} (c - c_0) v_r\} + \{(N_r - m x_G u_r) r + \frac{1}{2} N_{\delta} (c - c_0) r\} + N_{\delta} \delta + N_{r^2 v_r} r^2 v_r + N_{e^3} e^3 \\ f_4 = (m - Y_{\dot{v}_r}) (I_z - N_{\dot{r}}) - (m x_G - N_{\dot{v}_r}) (m x_G - Y_{\dot{r}}) \end{cases} \quad (12)$$

where e is the effective rudder angle given by Eq. (13). c is the weighted average flow speed over the rudder. It is defined by Eq. (14).

$$e = \delta \frac{v}{c} + \frac{rL}{2c} \quad (13)$$

$$c = \sqrt{\frac{A_p}{A_R} [(1 - \omega) u_r + k u_{A_{\infty}}]^2 + \frac{A_R - A_p}{A_R} (1 - \omega)^2 u_r^2} \quad (14)$$

where $u_{A_{\infty}}$ is the induced axial velocity far behind the propeller disk, which given by

$$u_{A_{\infty}} = -(1 - w) u + \sqrt{(1 - w)^2 u^2 + \frac{8}{\pi} K_T (nD)^2} \quad (15)$$

The $20^\circ - 20^\circ$ zigzag manoeuvre simulation was carried out using the equation (9) (Hinostroza et.al 2017). The rudder angle and heading angle are recorded, as shown in Figure.5.

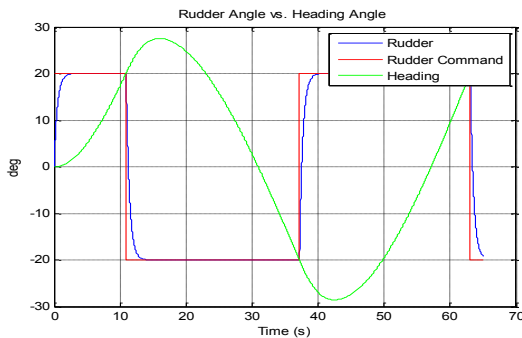


Figure 5. The $20^\circ - 20^\circ$ zigzag manoeuvre simulation

in which, acceleration of surge, sway and yaw is defined by:

$$\begin{cases} \dot{u}_r = \frac{f_1}{m - X_{\dot{u}_r}} \\ \dot{v}_r = \frac{1}{f_4} [(I_z - N_{\dot{r}}) f_2 - (m x_G - Y_{\dot{r}}) f_3] \\ \dot{r} = \frac{1}{f_4} [(m - Y_{\dot{v}_r}) f_3 - (m x_G - N_{\dot{v}_r}) f_2] \end{cases} \quad (11)$$

To design the heading controller, Nomoto model is a good option due to its simple structure. It is given by:

$$\begin{cases} \dot{\psi} = r \\ T\dot{r} + r = K\delta_R \end{cases} \quad (16)$$

The values of K and T can be calculated by analysing the ship behaviour during zigzag manoeuvres (Clarke, 2003; Journée 2001). In the following part, a system identification (Ljung, 1987) method is employed to find the values of K and T from the zigzag manoeuvre simulation data.

System identification is a technology for parameters estimation. It has been widely used for ship motion modelling (Sutulo and Guedes Soares 2014, Perera et al. 2015, Xu and Guedes Soares, 2016a). Recently a robust method, based on Support Vector Machine (Luo and Zou, 2009; Zhang and Zou, 2011; Luo, et al, 2014, 2016) was applied to identify the ship manoeuvring model and performed satisfactorily.

For parameter estimation, support vector machine gives a general approximation function form:

$$y = w^T \cdot \Phi(x) + b \quad (17)$$

where x is the input vector, $x \in \mathfrak{R}^n$, y is the output data, $y \in \mathfrak{R}$. $\Phi(\cdot)$ is a nonlinear mapping function, which is mapping the input data to a high dimensional feature space. To get the optimal parameters, a cost function is defined as following:

$$\begin{cases} \min_{w,b,e} f(w,e) = \frac{1}{2}w^T w + \frac{1}{2}C \sum_{i=1}^l e_i^2 \\ \text{subject to: } y_i = w^T \cdot \Phi(x_i) + b + e_i \end{cases} \quad (18)$$

where, e_i is error variables, and C is the regularization factor. A Lagrangian function is defined as:

$$\mathcal{L}(w,b,e,\alpha) = \frac{1}{2}w^T w + \frac{1}{2}C \sum_{i=1}^l e_i^2 - \sum_{i=1}^l \alpha_i [w^T \cdot \Phi(x_i) + b + e_i - y_i] \quad (19)$$

where α_i are the Lagrange multipliers. Compute the derivatives of (19) with respect to w, b, e, α :

$$\begin{cases} \frac{\partial \mathcal{L}}{\partial w} = 0 \rightarrow w = \sum_{i=1}^l \alpha_i \Phi(x_i) \\ \frac{\partial \mathcal{L}}{\partial b} = 0 \rightarrow \sum_{i=1}^l \alpha_i = 0 \\ \frac{\partial \mathcal{L}}{\partial e_i} = 0 \rightarrow \alpha_i = C e_i \\ \frac{\partial \mathcal{L}}{\partial \alpha_i} = 0 \rightarrow w^T \cdot \Phi(x_i) + b + e_i - y_i = 0 \end{cases} \quad (20)$$

then eliminate the variables w and e_i from the equations (20), LS-SVM model for function estimation yields

$$y(x) = \sum_{i=1}^l \alpha_i K(x, x_i) + b \quad (21)$$

where $K(\cdot, \cdot)$ is an inner product function. The kernel must be a positive definite kernel and must satisfy the Mercer condition (Mercer, 1909).

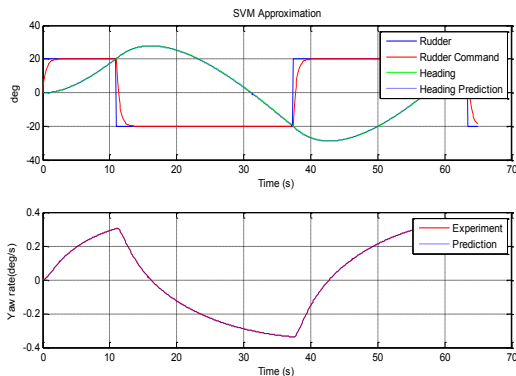


Figure 6. Prediction of 20° - 20° Zigzag manoeuvre

Considering the Nomoto model, the input sequence, $x = [r_k, \delta_k]$, is constructed. $y = [r_{k+1}]$ is output data. The regularization factor $C = 2544$ (Luo et al., 2016) is chosen. The Nomoto time and gain constants are the parameters to be estimated. The 20° - 20° Zigzag test is chosen as training data. The obtained for K and T are: K

$= 0.1807$ and $T = 7.3970$. In Figure. 6, the identification and experimental heading curves are in very good agreement.

4. HEADING AUTOPILOT DESIGN

According to the previous discussion, the PID heading controller is designed and the controller gains are calculated (Xu et al. 2017). Assuming that ψ is measured by a compass, consider the PID controller law:

$$\tau_N(s) = \tau_{PID}(s) = K_p(\psi_d - \psi) - K_d\dot{\psi} + K_i \int_0^t (\psi_d - \psi(\tau)) d\tau \quad (22)$$

where $K_p > 0$, $K_d > 0$ and $K_i > 0$ are the regulator design parameters. Applying this control law to Nomoto 1st order model (Eq. 16), the closed-loop characteristic equation can be obtained:

$$T\sigma^3 + (1 + KK_d)\sigma^2 + KK_p\sigma + KK_i = 0 \quad (23)$$

Applying Routh's stability criterion, another simple intuitive way to do this is by noticing that δ can be written as (Fossen, 2011):

$$\tau_N(s) = \tau_{PID}(s) = K_p(1 + T_d s + \frac{1}{T_i s})(\psi_d - \psi) \quad (24)$$

A continuous-time representation of the controller is

$$\tau_N(s) = \tau_{PID}(s) = K_p(\psi_d - \psi) + K_d(\dot{\psi}_d - \dot{\psi}) + K_i \int_0^t (\psi_d - \psi(\tau)) d\tau \quad (25)$$

where τ_N is the controller yaw moment, $K_d = K_p T_d$, and $K_i = K_p / T_d$. The controller gains can be found by pole placement in terms of the design parameters ω_n and ζ , though:

$$\begin{aligned} K_p &= \omega_n^2 T / K > 0 \\ K_d &= (2\zeta\omega_n T - 1) / K > 0 \\ K_i &= \omega_n^3 T / (100K) > 0 \end{aligned}$$

where ω_n is the natural frequency and ζ is the relative damping ratio of the 1st system. In this case, $\omega_n = 1$ rad/s and critical damping $\zeta = 1$. Thus, the following controller gains are obtained: $K_p = 40.9353$, $K_d = 76.3365$ and $K_i = 0.41$.

To achieve accurate and rapid course changing manoeuvres, a feed forward term can be applied to the controller. The PID- controller for full state feedback is given by:

$$\tau_N(s) = \tau_{FF}(s) + K_p(1 + T_d s + \frac{1}{T_i s})(\psi_d - \psi) \quad (26)$$

where τ_{FF} is a feedforward term to be decided. Using Nomoto's first-order model as basis for feedforward, suggests that reference feedforward should be included according to

$$\tau_{FF}(s) = \frac{T}{K} \dot{r}_d + \frac{1}{K} r_d \quad (27)$$

5. SIMULATIONS

In this section, simulation tests will be carried out to validate the performance of proposed optimal PLOS guidance law.

The optimal value of parameter p and q will be obtained using genetic algorithms. The cost function was defined in Eqs. (6-7) considering the comprehensive effect of the total cross-track errors and total control efforts. During the simulation, the program can converge to the optimal values very fast and then keep stable. It indicates that the GA can find the global optimal values. The optimal parameter p is 0.4528 q is 0.5473. When another cost function is chosen, the optimal parameter p is 0.3795 and q is 0.6210.

As presented in Figure.7, the trajectories of autonomous surface vehicles using GA-PLOS guidance law are more practical and reasonable. The cross-track error is not the minimum, but it is the optimal value in considering the total control effort, which plays an important role in the autonomous vehicles. GA-PLOS guidance law based on cost function 2 can also generated a reasonable trajectory. It can control the ship to follow the path without the unnecessary zigzag and overshoot. It can also minimise the heading errors, which is the input for the controller of autonomous surface vehicle.

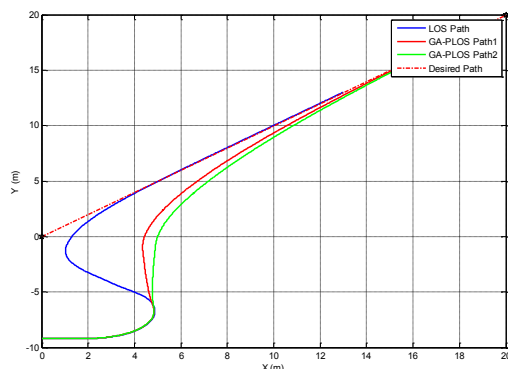


Figure 7. The trajectories of autonomous surface vehicles based on LOS and PLOS guidance law

Figure 8 presents the cross-track error, heading error and deflected rudder angle obtained using the classical LOS and GA-PLOS with different optimal parameters. From

this figure, the GA-PLOS can minimise the heading errors and control efforts significantly. Control efforts can be measured using the deflected rudder angle. In figure 8, the GA-PLOS with the parameters obtained using the cost functin2 can get a smaller heading errors, as showed in figure 8.

Figure 9 presented the velocity of surge, sway and yaw, and the drift angle of autonomous surface ship model using the guidance laws, which are discussed in the previous sections. During simulations, the surge velocity was assumed to be constant. As shown in figure 9, GA-PLOS guidance law can response the velocity of sway more quickly and can also avoid the oscillation, which is very important for underactuated surface vehicle. The oscillation of sway velocity always results the cross-track errors and cost more energy. In this figure, the GA-PLOS guidance law can also minimise the rate of yaw and drift angle.

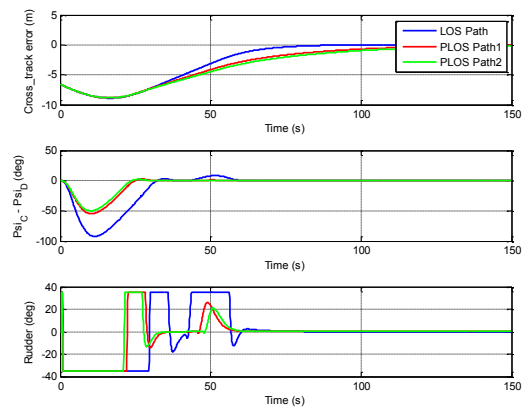


Figure 8. The cross-track error, heading error and deflect rudder angle of autonomous surface vehicle based on LOS and PLOS guidance law

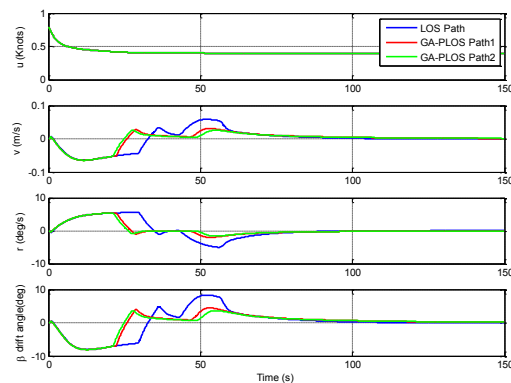


Figure 9 the velocity of surge, sway and yaw and the drift angle of autonomous surface vehicle using LOS and PLOS guidance law

A complex trajectory is defined to test the performance of GA-PLOS guidance law (Hinostrroza et.al 2018). A new simulation has been carried out to compare the performance of the classical LOS and GA-PLOS. The

path include 5 way-points. The desired speed is kept constant with a value of 0.4 knots, which corresponds to a Froude number $F_n = 0.0372$. The way-points are given by

$$\begin{aligned} \text{Wp1} &= (0,0), & \text{Wp2} &= (20,20), & \text{Wp3} &= (-20,10), \\ \text{Wp4} &= (-25,40), & \text{Wp5} &= (25,60). \end{aligned}$$

The simulation results are presented in Figure.10, which shows that GA-PLOS can guide the autonomous surface vehicle to follow the predefined path with good accuracy. The trajectory generated by the GA-PLOS is more practical and with less control effort and can avoid the zigzags and overshoot of the path.

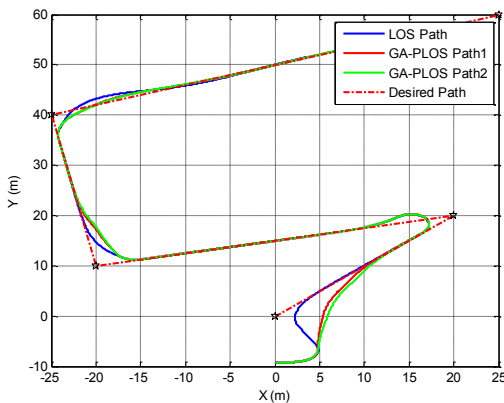


Figure 10. x-y plot of the simulated and desired geometrical path

Figure 11 shows the cross-track errors, heading errors and deflected rudder angles. In the figure, the GA-PLOS can minimise the cross-track errors with a slow speed. But GA-PLOS minimise the heading errors especially when the vehicle is far away from the desired path, it also means that the autonomous vehicles need to take a more effort to return to the path. From the last part of figure 11, GA-PLOS only need to spend less control effort to guide the vehicles to follow the predefined path.

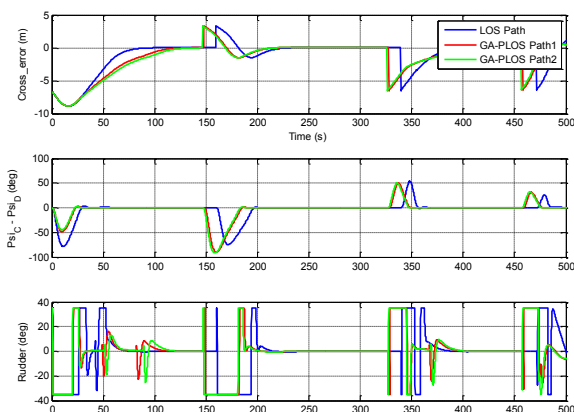


Figure 11. The cross track error, $\psi - \psi_d$ and deflected rudder angle in the process of following the trajectory

From Table 3-4 presented the statistics properties for both traditional line of sight and GA-PLOS guidance

laws. The GA-PLOS have a better performance since it exhibits lower mean and deviation of heading errors and rudder angle.

Figure 12 presented the sway velocity, yaw rate and the drift angle when the autonomous vehicle following the trajectory. From this figure, the sway velocity of the vehicle using the GA-PLOS guidance law is more stable. It also means that GA-PLOS can avoid the overshoot, which can be confirmed during the last transition part of the trajectory, as showed in the figure 10. GA-PLOS can also make the yaw rate and drift angle more stable. From the above discussion, the GA-PLOS can minimise the cross-track errors and guide the ship to converge to the predefined path, and can also minimise the heading error with a less control efforts. It can make the velocity of sway and rate of yaw smoother and avoid the unnecessary oscillations.

Table 3. The mean value of LOS and GA-PLOS

Data Type	LOS	GA-PLOS1	GA-PLOS2
$ y_e $ [m]	1.239	1.451	1.516
$ \psi_d - \psi $ [deg]	6.315	5.852	5.838
$ \delta_R $ [deg]	8.714	7.884	7.969

Table 4. The standard deviation of LOS and GA-PLOS

Data Type	LOS	GA-PLOS1	GA-PLOS2
$ y_e $ [m]	2.225	2.279	2.300
$ \psi_d - \psi $ [deg]	16.97	16.23	16.29
$ \delta_R $ [deg]	13.84	13.05	13.17

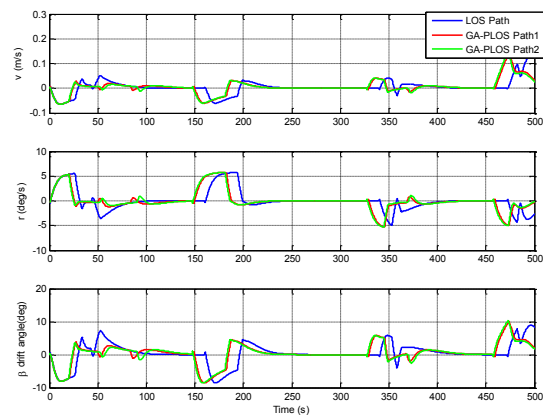


Figure 12. The sway velocity, yaw rate and drift angle in the process of following the trajectory

6. CONCLUSIONS

An optimized path-following algorithm aims at minimising the control energy was proposed for way-points tracking of a marine surface ship model. The modified version of the nonlinear Abkowitz model was introduced briefly. Least square support vector machine has been used to estimate the

parameters of the Nomoto model based on the zig-zag manoeuvring data. A combined feedforward and feedback PID controller was developed for the heading control. An optimal path-following guidance law was proposed to minimize the total cross-track errors and total control efforts by combining pure pursuit and line of sight guidance law. A global optimization algorithm was employed to search the regularization factors, which are the trade-off between the total cross-track errors and total control energy. The simulation tests have been carried out to demonstrate the performance of the proposed algorithm. The results are compared with the classical LOS guidance law. From the simulation, the GA-PLOS can guide the vehicles to follow the predefined path successfully. The proposed guidance law is an effective and practical guidance law for autonomous surface vehicles.

7. ACKNOWLEDGEMENTS

This work was performed within the Strategic Research Plan of the Centre for Marine Technology and Ocean Engineering (CENTEC), which is financed by Portuguese Foundation for Science and Technology (Fundação para a Ciência e Tecnologia-FCT) under contract UID/Multi/ 00134/2013-LISBOA-01-0145-FEDER-007629.

8. REFERENCES

1. ABKOWITZ M.A. 1980. *Measurement of hydrodynamic characteristics from ship maneuvering trials by system identification*. SNAME Transactions, 88, pp. 283-318.
2. BREIVIK, M. and FOSSEN, T. I. 2009. *Guidance Laws for autonomous underwater vehicles*. Underwater Vehicles, A. V. Inzartsev, Ed. Vellore, India: INTECH Education Publishing, pp. 51-76, ch. 4.
3. BREIVIK, M. and FOSSEN, T. I. 2008. *Guidance Laws for Planar Motion Control*. Proceeding of the 47th IEEE Conference on Decision and Control, Cancun, Mexico, pp. 570-576.
4. CAHARIJA, W., PETTERSEN, K.Y., CALADO, P., BRAGA, J., 2015. *A Comparison Between the ILOS Guidance and the Vector Field Guidance*. IFAC-PapersOnLine 48, 89-94.
5. CLARKE D., 2003. *The Foundations of Steering and Maneuvering*. In: Proceedings of Sixth Conference on Maneuvering and Control of Marine Crafts (MCMC' 2003), Girona, Spain, pp. 2-16.
6. CHEN, C., SHIOTANI, S. and SASA K. 2013. *Numerical ship navigation based on weather and ocean simulation*, Ocean Engineering, Vol. 69, No. 1, pp. 44-53.
7. FREW E. W. LAWRENCE D. A. and MORRIS S. 2008. *Coordinated Standoff Tracking of Moving Targets using Lyapunov Guidance Vector Fields*, Journal of Guidance, Control, and Dynamics, vol. 31, pp. 17.
8. FOSSEN, T., BREIVIK, M., SKJETNE, R., 2003. *Line-of-sight path following of underactuated marine craft*, in: Proceedings of the 6th IFAC MCMC, Girona, Spain. pp. 244-249.
9. FOSSEN, T. I. 2002. *Marine control systems: Guidance, navigation and control of ships, rigs and underwater vehicles*, Marine Cybernetics. Trondheim, Norway.
10. FOSSEN, T. I. 2011. *Handbook of marine craft hydrodynamics and motion control*, Wiley Publishers.
11. FOSSEN, T. I., K. Y. PETTERSEN and R. GALEAZZI. 2015. *Line-of-Sight Path Following for Dubins Paths with Adaptive Sideslip Compensation of Drift Forces*. IEEE Transactions on Control Systems Technology, Vol. 23, No. 2, pp. 820-827.
12. HINOSTROZA, M. A., H. T. XU, GUEDES SOARES, C. "Experimental and numerical simulations of zig-zag manoeuvres of a self-running ship model," in Maritime Transportation and Harvesting of Sea Resources, Guedes Soares, C. & Santos, T. A., Ed. London, UK: Taylor & Francis Group, 2017, pp. 563-570.
13. HINOSTROZA, M. A., H. T. XU, GUEDES SOARES, C. "Path-planning and path-following control system for autonomous surface vessel," in Maritime Transportation and Harvesting of Sea Resources, Guedes Soares, C. & Santos, T. A., Ed. London, UK: Taylor & Francis Group, 2018, pp. 991-998.
14. JOURNÉE, J.M.J. 2001. *A simple method for determining the manoeuvring indices k and t from zigzag trial data*. DUT-SHL Technical Report 0267, Delft, Netherlands.
15. JINGSONG, Z., PRICE, W.G., WILSON, P.A., 2008. *Automatic Collision Avoidance Systems: Towards 21st Century*. Department of Ship Science, University of Southampton.
16. LOE, Ø. A. G. 2008. *Collision Avoidance for Unmanned Surface Vehicles*, Master Thesis, Norwegian University of Science and Technology.
17. LUO, W., GUEDES SOARES, C., ZOU, Z., 2016. *Parameter Identification of Ship Maneuvering Model Based on Support Vector Machines and Particle Swarm Optimization*. J. Offshore Mech. Arct. Eng. 138, 31101.
18. LEKKAS, A. M. and FOSSEN, T. I. 2013. *Line-of-Sight Guidance for Path Following of Marine Vehicles*. Advanced in Marine Robotics, LAP LAMBERT Academic Publishing (O. Gal, Ed.), pp. 63-92.
19. LEKKAS, A. M. and FOSSEN, T. I. 2014. *Integral LOS Path Following for Curved Paths*

- Based on a Monotone Cubic Hermite Spline Parametrization. IEEE Transactions on Control Systems Technology, Vol. 22, No. 6, pp. 2287-2301
20. LIM S. L. JUNG W. and BANG H. 2014. *Vector field guidance for path following and arrival angle control*. 2014 International conference on unmanned aircraft systems, Orlando, USA. pp.329-338
 21. LIU, L., WANG, D., PENG, Z., 2016a. *Path following of marine surface vehicles with dynamical uncertainty and time-varying ocean disturbances*. Neurocomputing 173, 799–808.
 22. LIU, L., WANG, D., PENG, Z., WANG, H., 2016b. *Predictor-based LOS guidance law for path following of underactuated marine surface vehicles with sideslip compensation*. Ocean Eng. 124, 340–348.
 23. LJUNG L. 1987. *System identification: theory for the user*, Prentice-Hall, Englewood Cliffs, N J.
 24. LUO, W.L. GUEDES SOARES C. and ZOU, Z.J. 2016. *Parameter identification of ship manoeuvring model based on particle swarm optimization and support vector machines*. Journal of Offshore Mechanics and Arctic Engineering. 138: 031101-1 - 031101-8.
 25. LUO, W.L., MOREIRA, L. and GUEDES SOARES, C. 2014, *Manoeuvring Simulation of Catamaran by Using Implicit Models Based on Support Vector Machines*, Ocean Engineering, Vol. 82, pp. 150-159.
 26. LUO, W.L. and ZOU, Z.J. 2009. *Parametric identification of ship manoeuvring models by using support vector machines*. J. Ship Res. vol. 53 (1), pp. 19–30
 27. MELANIE M. 1996. *An Introduction to Genetic Algorithms*. Cambridge, MA: MIT Press.
 28. MOREIRA, L. and GUEDES SOARES, C. 2011a. *Guidance and Control of Autonomous Vehicles*. Guedes Soares, C. Garbatov Y. Fonseca N. and Teixeira A. P., (Eds.). Marine Technology and Engineering. London, UK: Taylor and Francis Group; pp. 503-520.
 29. MOREIRA L. and GUEDES SOARES, C. 2011b. *Autonomous ship model to perform manoeuvring tests*, Journal of Maritime Research, 8(2) pp. 29-46
 30. MOREIRA L. FOSSEN, T.I. and GUEDES SOARES, C. 2007. *Path following control system for a tanker ship model*, Ocean Engineering, 34, pp. 2074-2085
 31. PERERA, L. P.; CARVALHO, J. P., and GUEDES SOARES, C. 2011. *Fuzzy-logic based decision making system for collision avoidance of ocean navigation under critical collision conditions*. Journal of Marine Science and Technology. 16 (1): 84–99.
 32. PERERA, L. P.; OLIVEIRA, P., and GUEDES SOARES, C. 2015. *System Identification of Nonlinear Vessel Steering*. Journal of Offshore Mechanics and Arctic Engineering. 137:031302-1 - 031302-7.
 33. PERERA L. P. MOREIRA L. SANTOS F. P. FERRARI V. SUTULO S., GUEDES SOARES C. 2012. *A Navigation and Control Platform for Real-Time Manoeuvring of Autonomous Ship Models*. Proceedings of the 9th IFAC Conference on Manoeuvring and Control of Marine Craft (MCMC2012), Arenzano, Italy
 34. PERERA, L. P.; FERRARI, V.; SANTOS, F. P.; HINOSTROZA, M. A., and GUEDES SOARES, C. 2015. *Experimental Evaluations on Ship Autonomous Navigation and Collision Avoidance by Intelligent Guidance*. IEEE Journal of Oceanic Engineering. 40 (2) :374-387
 35. SUTULO, S. and GUEDES SOARES, C. 2005. *Numerical Study of Some Properties of Generic Mathematical Models of Directionally Unstable Ships*. Ocean Engineering. 32(3-4):485-497.
 36. SUTULO, S. and GUEDES SOARES, C. 2014. *An Algorithm for Offline Identification of Ship Manoeuvring Mathematical Models after Free-Running Tests*. Ocean Engineering; 79:10-25.
 37. SUTULO S. MOREIRA L. and GUEDES SOARES, C. 2002. *Mathematical models for ship path prediction in manoeuvring simulation systems*, Ocean Engineering, 29, pp. 1-19
 38. VETTOR, R. and GUEDES SOARES, C. 2015. *Multi-objective evolutionary algorithm in ship route optimization*, Maritime Technology and Engineering, Guedes Soares, C. and Santos T.A. (Eds.), Taylor and Francis Group, London, UK, pp. 865-876
 39. WANG, N., SUN, Z., YIN, J., ZHENG, Z., 2017. *Surge-varying LOS based path following control of underactuated marine vehicles with accurate disturbance observation*, in: 2017 IEEE 7th International Conference on Underwater System Technology: Theory and Applications (USYS). IEEE, pp. 1–6.
 40. XU, H., GUEDES SOARES, C., 2016a. *Vector field path following for surface marine vessel and parameter identification based on LS-SVM*. Ocean Eng. 113, 151–161
 41. XU, H. T., GUEDES SOARES, C. “Waypoint-following for a marine surface ship model based on vector field guidance law,” in Maritime Technology and Engineering 3, vol. 1, Guedes Soares, C. and Santos, T. A., Eds. London, UK: Taylor & Francis Group, 2016b, pp. 409–418.
 42. XU, H., GUEDES SOARES, C., 2015. *An optimized path following algorithm for a surface ship model*. Towar. Green Mar. Technol. Transp. Taylor & Francis, 151–158.
 43. XU, H. T., M. A. HINOSTROZA, GUEDES SOARES, C. “A hybrid controller design for ship autopilot based on free-running model test,” in Maritime Transportation and Harvesting of Sea Resources, Guedes Soares, C. & Santos, T.

- A., Ed. London, UK: Taylor & Francis Group, 2017, pp. 1051–1059.
44. XU, H.T., HINOSTROZA, M.A., GUEDES SOARES,C., 2018. *Estimation of Hydrodynamic Coefficients of a Nonlinear Manoeuvring Mathematical Model with Free-Running Ship Model Tests*. *Int. J. Marit. Eng.* (Accepted)
45. ZHANG, X. G. AND ZOU, Z. J. 2011. *Identification of Abkowitz model for ship manoeuvring motion using ε -support vector regression*. *J. Hydrodynamics* Vol.23 (3), pp. 353–360
46. ZARCHAN P. 1990. *Tactical and Strategic Missile Guidance*. In *Progress in Astronautics and Aeronautics*, AIAA Paper Vol. 124.